Journal of Food Composition and Analysis 131 (2024) 106262

Contents lists available at ScienceDirect

Journal of Food Composition and Analysis

journal homepage: www.elsevier.com/locate/jfca

Sensitive detection of ofloxacin by lateral flow immunoassay based on Prussian blue nanoparticles and colloidal gold

Can Li [a,c], Shuangshuang Cui [a,c], Jian Zhang [a,c,d], Yunfeng Zhao [a,d], Xiayu Peng [b,*], Fengxia Sun [a,c,d,**]

[a] School of Food Science and Technology, Shihezi University, Shihezi, Xinjiang 832003, China
[b] College of Animal Science and Technology, Shihezi University, Shihezi, China
[c] Key Laboratory of Agricultural Product Processing and Quality Control of Specialty(Co-construction by Ministry and Province), School of Food Science and Technology, Shihezi University, Shihezi, China
[d] Key Laboratory for Food Nutrition and Safety Control of Xinjiang Production and Construction Corps , School of Food Science and Technology, Shihezi University, Shihezi, China

ARTICLE INFO

Keywords:
Lateral flow immunoassay
Prussian blue nanoparticles
Golloidal gold
Ofloxacin
Fish
Visual detection method

ABSTRACT

In this paper, Prussian blue nanoparticles (PBNPs) and colloidal gold (AuNPs) were synthesized by solvothermal method and trisodium citrate reduction method respectively, and two lateral flow immunoassay (LFIA) methods for the detection of ofloxacin (OFL) in fish were established. The larger particle size and superior optical properties of PBNPs make the sensitivity of PBNPs-LFIA higher than that of AuNPs-LFIA. In the process of establishing the assay, we found that the amount of antibody required for PBNPs-LFIA is 1/3 of that for AuNPs-LFIA, and the amount of probe is 1/2 of that for AuNPs-LFIA, suggesting that PBNPs-LFIA is able to save the amount of antibody and greatly reduce the cost of the assay.The detection limit of PBNPs-LFIA for OFL was 0.064 ng mL^{-1}, which was 2.3 times lower than that of AuNPs-LFIA, and the visual detection limit and elimination value of PBNPs-LFIA were also lower than that of AuNPs-LFIA.In addition, the recoveries of two established LFIAs for the determination of OFL in fish were 84.8 %-116.3 %, and the coefficient of variation was less than 10 %. Therefore, PBNPs are a potential LFIA probe marker.

1. Introduction

Fluoroquinolones (FQs) are broad-spectrum antibacterial drugs that target DNA gyrase and topoisomerase IV (Jin et al., 2023). In Gram-negative bacteria, FQs target DNA gyrase, inhibiting its activity and achieving antibacterial effects, and in Gram-positive bacteria, FQs target topoisomerase IV inhibiting its activity and interfering with DNA replication (Jirachaya et al., 2023). Ofloxacin (OFL) is a fluoroquinolone that inhibits the activity of bacterial DNA gyrase. It is a low-cost veterinary drug with a broad antibacterial spectrum, high efficiency, low toxicity, and strong tissue penetration. Its antibacterial effect is nearly 1000 times that of sulfonamides (Qureshi et al., 2016). OFL has become a crucial anti-infective drug in veterinary clinics and aquaculture. However, improper drug use during aquaculture and production can lead to the transformation and enrichment of FQs in animals, resulting in drug residues in animal food (Andreu, 2007). Residual FQs can cause harmful toxic effects on the central nervous system, liver and kidneys when ingested and absorbed through the food chain (Rodriguez-Mozaz et al., 2020). In addition, excessive use of antibiotics will also cause environmental pollution and the emergence of drug-resistant pathogens. For the detection of FQs in food, traditional detection methods include high performance liquid chromatography (HPLC), enzyme-linked immunosorbent assay (ELISA) and electrochemical analysis (Liao et al., 2023), but all of them have shortcomings such as complicated operation, huge equipment and long detection time. Therefore, it is of great significance to develop a rapid detection method with simple equipment and high sensitivity.

Lateral Flow Immunoassay (LFIA) is a simple, economical and convenient method for the rapid detection of various substances (Rana et al., 2024). Gold nanoparticles (AuNPs) are currently the most widely used markers in lateral flow immunoassays (Anfossi et al., 2010; Cavalera et al., 2021; Nardo et al., 2021). It is widely used by researchers to

* Corresponding author.
** Corresponding author at: School of Food Science and Technology, Shihezi University, Shihezi, Xinjiang 832003, China.
E-mail addresses: pengxy@shzu.edu.cn (X. Peng), shzsfx@163.com (F. Sun).

https://doi.org/10.1016/j.jfca.2024.106262
Received 2 February 2024; Received in revised form 29 March 2024; Accepted 14 April 2024
Available online 20 April 2024

detect a variety of disease-causing microorganisms and pathogens (Huang et al., 2023). However, the weak optical properties of colloidal gold and low biomolecule binding rate lead to the low sensitivity of traditional gold-labeled lateral flow chromatography test strips, making it difficult to meet the demand for highly sensitive and rapid detection of trace hazards (Yang et al., 2023). To address this issue, researchers have been exploring alternative materials to replace AuNPs, including quantum dots, fluorescent microspheres, and chemiluminescent carbon nanodots (Yin et al., 2024; Wang et al., 2023). However, the preparation of these labeling materials is complicated and generally requires a long time as well as special equipment. Prussian blue nanoparticles (PBNPs) have gained significant attention in the field of biomedicine due to their economic and easy synthesis (Busquets et al., 2020; Qin et al., 2018). The preparation of PBNPs is relatively simple and has stable performance. They can provide an excellent specific surface area by controlling particle and pore size (Qiu et al., 2019; Feng et al., 2013). Additionally, their unique optical properties make them suitable as signaling probes, producing clear blue bands during LFIA detection (Hendrickson et al., 2023). In addition, as a metal-organic framework material, the framework structure of PBNPs can effectively protect antibodies, and the affinity of PBNPs for biological macromolecules enables antibodies to be connected with them through electrostatic adsorption, which provides a convenient and simple method for preparing PBNPs-mAb. During the assay process, the sample matrix, organic solvents, and temperature can significantly impact the results. However, previous studies have shown that PBNPs coupling are highly immune to interference and remain stable even when conditions change (Juliana et al., 2019).

Currently, Prussian blue nanoparticles have been widely used as a superior labeling material in lateral flow immunochromatographic assays (Tian et al., 2020; Liu et al., 2020; Zhang et al., 2022). Zhao et al. used Prussian blue nanoparticles as markers to establish a sensitive lateral flow immunoassay for the detection of leptin in pork (Zhao et al., 2018). In addition, PBNPs have good peroxidase-like activity and can catalyze H_2O_2 to change the color of TMB. The researchers used this property of PBNPs to amplify the test strip signal (Ren et al., 2022). He et al. used Prussian blue nanoparticles in the detection of glycocholic acid and achieved signal amplification when used in combination with TMB (He et al., 2020). PBNPs can also be combined with magnetic nanomaterials to prepare magnetic Prussian blue nanoparticles. Liang et al. established test strips for the detection of agonists in pig urine and pork. Magnetic Prussian blue can be used to enrich for the target to be detected in the sample during sample pretreatment and also to amplify the signal during detection (Liang et al., 2023). In addition, PBNPs degrade and fade under alkaline conditions, thereby diminishing the color of the T and C lines in immunochromatographic strips. Based on this property, PBNPs can be used to establish a competitive lateral flow immunochromatographic assay, which can achieve improved sensitivity. Bu et al. proposed a competitive immunochromatographic test strip based on a signal amplification strategy assisted by the decomposition of PBNPs, which resulted in an 8-fold reduction in LOD compared to conventional colloidal gold test strips (Bu et al., 2021).

In this study, stabilized PBNPs were synthesized by solvothermal method using polyvinylpyrrolidone (PVP-K30) as a stabilizer, and then the detection probes were obtained by electrostatic adsorption combined with anti-OFL mAb. A competitive lateral flow immunochromatographic assay was established using dark blue PBNPs as a signal label, which can be used to detect OFL in samples with high sensitivity. In addition, a conventional AuNPs-LFIA method was established and compared with PBNPs-LFIA. The results showed that PBNPs-based LFIA could detect the target more sensitively and significantly improve the detection performance.

2. Experimental and methods

2.1. Materials and equipment

Trisodium citrate, potassium carbonate, potassium ferricyanide were purchased from Sigma-Aldrich (St. Louis, MO, USA).; Chloric acid, bovine serum albumin, ovalbumin and polyvinyl pyrrolidone (PVP-K30) was purchased from McLean Co. (China); PEG20000, boric acid and sodium tetraborate were purchased from Aladdin Co. (China). Anti-OFL mAb and OFL coating antigen (OFL-OVA) were prepared by the laboratory itself; goat anti-mouse IgG was purchased from Biodragon Co. (China). The standards of ofloxacin, ciprofloxacin, moxifloxacin, pefloxacin, enoxacin, gatifloxacin, norfloxacin and difluorofloxacin were purchased from Solaibao Co. (China). Sample pad treatment solution composition: Tris-HCl (0.05 M, pH 8.0) solution containing 0.15 M NaCl and 0.25 % TritonX-100. All the solutions were prepared with ultrapure water (resistivity: 18.2 MΩ-cm).

Glass cellulose membrane (RB65), absorbent pad (CH37K) and PVC bottom plate were all purchased from Shanghai Jinbiao Bio-Standard Technology Co. (China); NC membrane (Sartorius CN95) was purchased from Shanghai Jieyi Biotechnology Co. (China).

2.2. Preparation of PBNPs and PBNPs-mAb

PBNPs were synthesized according to a modification of the methodology of a previous study (Hu et al., 2012). First, 5 g of PVP-K30 pellets were dissolved in 40 mL of 0.01 M HCl solution. Then 0.25 g of $K_3[Fe(CN)_6]\cdot 3\ H_2O$ was added and stirring was continued for 1 hour to obtain a clear, transparent solution and the reaction was carried out at 80°C for 24 hours. At the end of the reaction, the compound was cooled and centrifuged at 6700× g for 25 min. The blue precipitate was collected from the bottom layer and washed three times with ethanol and ultrapure water and dried. The powder obtained consisted of Prussian blue nanoparticles.

The synthesis of PBNPs-mAb was modified (Feng et al., 2013). Add 5 μL of anti-OFL mAb to the PBNPs solution and mix. The mixture is then incubated for 1 hour at room temperature with shaking. At this point there may still be some sites on the surface of the PBNPs that are not bound to the antibody, so a solution of BSA (10 %, w/v) is added and the reaction is carried out for 1 hour to block these active sites. At the end of the reaction, the mixture was centrifuged at 5400×g for 30 min to collect the blue precipitate, which was resuspended to 1/10 of its original volume with resuspension solution.

2.3. Synthesis of AuNPs and AuNPs-mAb

AuNPs was obtained by reducing chloroauric acid with trisodium citrate (Zhang et al., 2019). Specific steps are in the supplementary material.

AuNPs-mAb was synthesized according to the previous research (Zhong et al., 2016). Specific steps are in the supplementary material.

2.4. Preparation of the test strips

The test strip is composed of a sample pad, NC film, absorbent paper, and PVC bottom plate. The NC membrane was coated with goat anti-mouse IgG (1.0 mg mL^{-1}) and OFL-OVA as control (C line) and test (T line) lines, respectively. The membrane was subsequently incubated at 37℃ for 2 hours. Cut the sample pads to a fixed size and soak them in the sample pad treatment solution for two hours, then dry them at 27℃ before use. This is because non-specific binding sometimes occurs during immunochromatography, which can reduce the accuracy of the experiment. By pretreating the sample pads, non-specific binding can be minimized and the specificity and sensitivity of the experiment can be improved. Next, the sample pad, NC film, and absorbent paper were sequentially pasted onto the PVC floor, ensuring an overlap of at least

2 mm between them. Finally, the assembled test strip was cut into 4 mm strips for later use.

2.5. Test procedure

The detection procedures of PBNPs-LFIA and AuNPs-LFIA are as follows: add 90 μL OFL standard (5 ng mL^{-1}) into the wells of 96-well microplates, then add 10 μL detection probe (PBNPs-mAb or AuNPs-mAb) and mix well, insert the test strip to react for 20 min. Finally, the test strips were removed and photographed using cell phone. The pictures were processed and analyzed using Image J to get the grayscale intensity of the bands on the test strip. At the same time, the same volume of PBS (0.01 M, pH 7.4) was used instead of OFL standard as negative control group.

2.6. Optimization of LFIA test conditions

The key influencing factors of two lateral flow immunoassays were optimized in order to improve the detection performance of both test strips, including the concentration of PBNPs (0.1, 0.2, 0.3, 0.4, 0.5 mg mL^{-1}), the amount of antibody label (2, 4, 6, 8, 10 μg), the dilution of PBNPs antibody (0×, 2×, 3×, 4×), the type of detection probe resuspension (BSA, PVP-K30, PEG20000), and the concentration of T line labeled OFL-OVA (0.2, 0.4, 0.6, 0.8, 1.0 mg mL^{-1}). AuNPs-LFIA was also optimized for the amount of K_2CO_3 used for labeling of AuNPs with the antibody (0, 2, 4, 6, 8 μL) as well as the particle sizes of the AuNPs (17 nm, 23 nm, 59 nm).

2.7. Performance evaluation of the LFIAs

2.7.1. Sensitivity

OFL standards were diluted to 0, 0.025, 0.05, 0.25, 0.5, 1, 2.5, 5 and 10 ng mL^{-1} with PBS (0.01 M, pH 7.4) to form eight concentration gradients. Standard curves for AuNPs-LFIA and PBNPs-LFIA were established according to the assay procedure described in 2.5. Afterwards, the data were analyzed using Origin software for nonlinear fitting with the concentration of the standard as the horizontal coordinate and the T line grayintensity as the vertical coordinate. In addition, a linear fit was performed using the logarithmic value of the concentration of the standard as the horizontal coordinate and the T line gray scale intensity as the vertical coordinate, and the linear equation of the standard curve was obtained (Liu et al., 2023; Cai et al., 2023). Each experiment was replicated three times. In addition, the limit of detection (LOD) was determined by 20 blank samples. LOD is the measured value of 20 blank samples + 3 × the standard deviation of the blank samples (Liu et al., 2022; Huang et al., 2023).

2.7.2. Specificity

To verify the specificity of LFIA, we selected seven other fluoroquinolones to test together with ofloxacin, namely ciprofloxacin, moxifloxacin, pefloxacin, enoxacin, gatifloxacin, norfloxacin and difluorofloxacin. Seven fluoroquinolones were diluted to 500 ng mL^{-1} with PBS (0.01 M, pH 7.4), and the OFL standard solution of 5 ng mL^{-1} was used as the positive control, and the test strips were photographed and analyzed for T line grayscale intensity using Image J. Each experiment was repeated three times.

2.7.3. Pretreatment of actual samples

The sample pretreatment method was referenced from previous study (Wang et al., 2015) and partially modified as follows: weigh 2.5 g of the fish sample in a 50 mL centrifuge tube, add 5 mL of PBS to the centrifuge tube and grind it to a pulp using a handheld homogenizer. The homogenizer was rinsed with 5 mL of PBS (0.01 M, pH 7.4) and the rinse solution was combined with the sample solution and centrifuged at 2200× g for 5 min. The supernatant was transferred to another centrifuge tube, the homogenizer and the previous centrifuge tube were rinsed with PBS (0.01 M, pH 7.4), and centrifugation was performed at 2200× g for 5 min again, and the supernatant was combined with the previous one and fixed to 25 mL and keep it for later use.

2.7.4. Recovery experiment

The accuracy and precision of the two test methods were evaluated by the recovery rate and coefficient of variation. Samples were analyzed by HPLC and determined to be free of OFL. Add 0.5 μg kg^{-1}, 2.5 μg kg^{-1} and 5 μg kg^{-1} OFL standard solution to the untreated samples, respectively, and then perform the detection according to the operation steps in 2.7.3, and set up three parallel experiments for each experimental group.

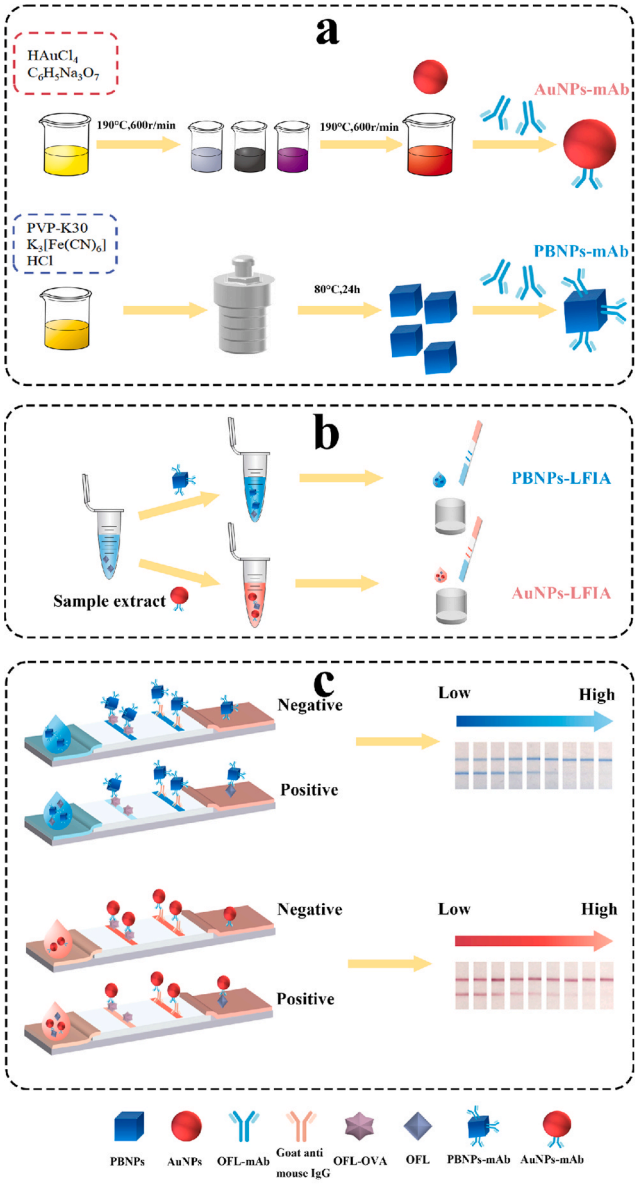

Fig. 1. Schematic illustration of PBNPs-LFIA and AuNPs-LFIA for OFL detection. (a) Synthetic process of PBNPs, PBNPs-mAb, AuNPs, AuNPs-mAb; (b) Schematic illustration of the detection process; (c) Detection principle of PBNPs-LFIA.

3. Results and discussion

3.1. Detection principle of LFIA

Fig. 1 illustrates the detection principle of LFIA. The detection target contained in the sample competes with OFL-OVA on the T line for binding with Ab in the detection probe. When the sample does not contain the target, the detection probe will bind to the OFL-OVA of the T line, forming a dark blue or red line; if the sample contains enough of the target, the detection probe will preferentially bind to the target. At this time, OFL-OVA does not bind to any probe, resulting in no color development in the T line. The degree of color development in the T line is inversely proportional to the concentration of the detection target in the sample.

3.2. Characterization of AuNPs and AuNPs-mAb probe

The results of transmission electron microscope (TEM) are shown in Fig. S1 (a). The results show that the synthesized AuNPs has uniform size and good dispersibility, and its particle size is about 23 nm (He et al., 2020). UV–vis absorption spectrum Fig. S1 (b) showed that the maximum absorption wavelength of AuNPs shifted from 521 nm to 527 nm; after coupling with anti-OFL mAb (Sunanda et al., 2017; Wolfgang et al., 2007). Compared to AuNPs-mAb, the zeta potential of AuNPs in Fig. 1(c) ranged from −70.2 mV to −55.3 mV, indicating successful coupling of AuNPs with the antibody.

3.3. Characterizations of PBNPs and PBNPs-mAb probes

The scanning electron microscopy (SEM) results in Fig. 2 show that the PBNPs have a cubic structure with a well-defined shape and uniform distribution, and the diameter of the particles is about 100 nm (Zakaria et al., 2015). The XRD result of Fig. 2(c) shows that the synthesized PBNPs has a good crystal structure, and its diffraction peak is consistent with the previous research, which indicates that the PBNPs is successfully synthesized (Hu et al., 2012; Hu et al., 2012). Fig. 2(d) Fourier transform infrared spectroscopy (FI-TR) shows that PBNPs and PBNPs-mAb have obvious tensile vibration around 2092 cm^{-1}, which may be due to the fact that PBNPs contain C≡N. Compared with PBNPs, PBNPS-mAb showed obvious tensile vibration in the amide ii band at 1500–1600 cm^{-1} and at 3294 cm^{-1}, indicating that PBNPS-mAb contained C-N, N-H and O-H groups, indicating that anti-OFL mAb was successfully coupled with PBNPs (Zakaria et al., 2015). Blanks are films that do not hold any substance in place. Fig. 2(e) UV–vis absorption spectrum showed that the maximum absorption wavelengths of PBNPs and PBNPs-mAb were 704 nm and 715 nm, respectively, and the maximum absorption wavelength of PBNPs-mAb was shifted, indicating that the antibody was successfully coupled with PBNPs. In addition, the change in zeta potential in Fig. 2(f) can also show that the antibody is successfully bound to PBNPs.

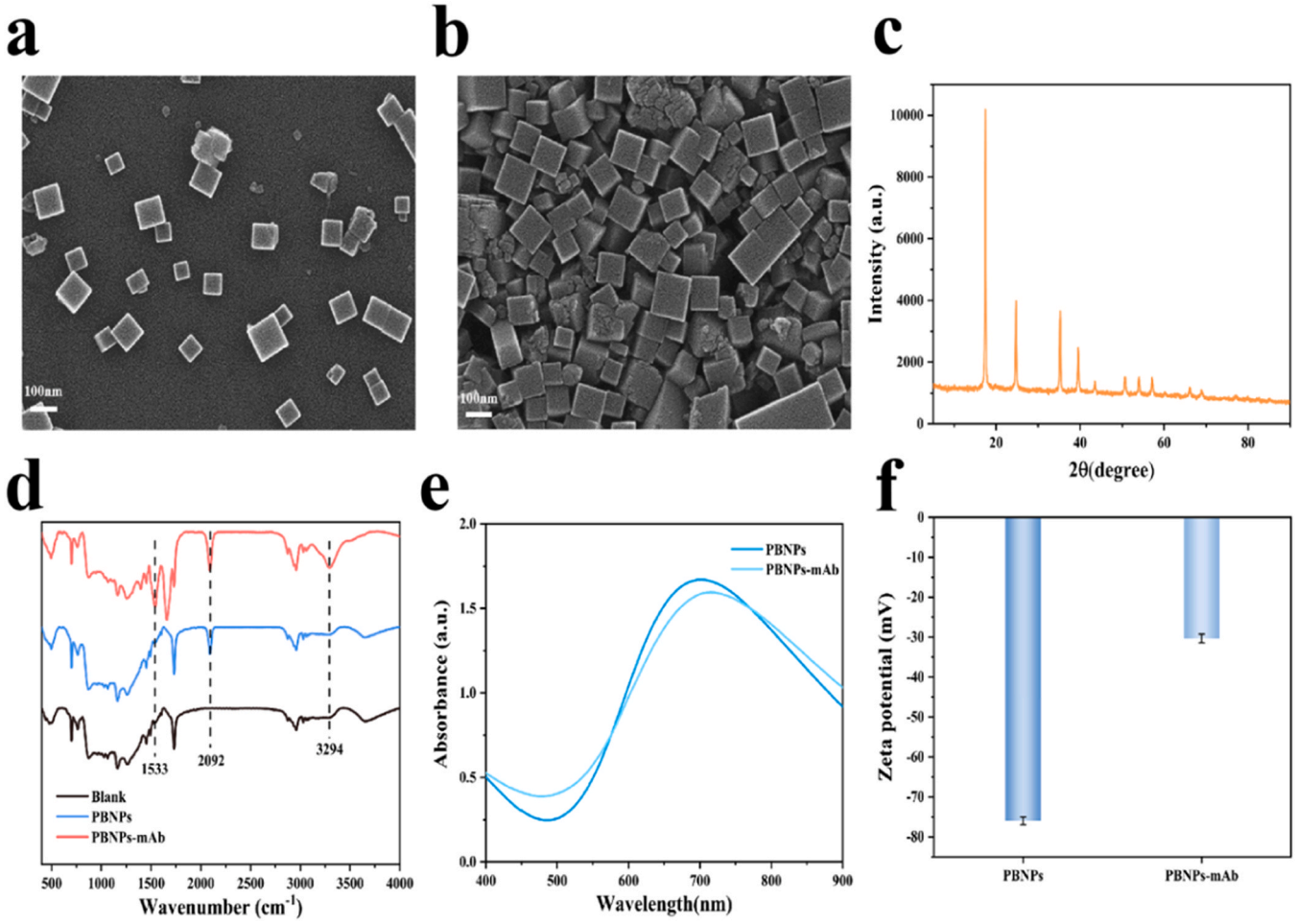

Fig. 2. Characterization results of PBNPs and PBNPs-mAb probe. (a, b) SEM image of PBNPs; (c) XRD spectra of PBNPs. (d) FT-IR spectra of PBNPs and PBNPs-mAb. (e) UV–vis absorption spectra of PBNPs and PBNPs-mAb. (f) Zeta potentials of PBNPs and PBNPs-mAb.

3.4. Optimization of detection conditions of PBNPs-LFIA

3.4.1. Optimization of PBNPs concentration

The concentration of the signal marker directly affects the detection sensitivity and background color of lateral flow immunoassay strips. The principle of optimizing the optimal concentration of PBNPs in the probe is to select a concentration that produces a clear blue band in the detection region and does not interfere too much with the background of the test strip, while still allowing the strip to have high sensitivity. As shown in Fig. 3(a), five PBNPs with different concentration gradients were selected. As the concentration of PBNPs increased, the colors of the C line and T line in the test strip also deepened. However, the particle size of PBNPs is large, and the increase in concentration will not be conducive to its flow on NC membrane, which will lead to the increase of background signal, which will greatly interfere with the processing of experimental data. When the concentration of PBNPs was 0.1 mg mL^{-1}, the background of the NC film was clean and has good sensitivity, so 0.1 mg mL^{-1} was selected as the best concentration of PBNPs.

3.4.2. Optimization of the best labeling amount of antibody in PBNPS-mAb

The detection principle of the immunostrips in this experiment is based on the competitive reaction to detect small molecules, so the amount of antibody labeled on the probe can greatly affect the sensitivity of the strips. We prepared PBNPs-mAb by adding 2, 4, 6, 8, and 10 μg of antibody per 1 mL of PBNPs solution, respectively. As demonstrated in Fig. 3(b), the color intensity of the C line and T lines increases as the amount of antibody labeling is raised from 2 μg to 10 μg. This is because as the amount of antibody labeling increases, more and more PBNPs-mAb is recognized and bound by OFL-OVA on the T line, which is trapped on the T line and forms a blue band. At the same time, the excess PBNPs-mAb will flow through the chromatography onto absorbent paper and bind to the secondary antibody on the C line to create a blue band. In the competitive test strip, the sensitivity of the test strip improves as the amount of antibody decreases. This is due to the increased competition between the coating antigen on the T line and the target (Zhang et al., 2011). In order to obtain better sensitivity under the condition of ensuring good T line color development, the addition of 2 μg of antibody per mL of PBNPs was set as the optimal test condition.

3.4.3. Optimization of dilution multiple of PBNPS-mAb detection probe

In a lateral flow immunoassay, the test probe flows chromatographically from the sample pad to the absorbent paper and, as it passes through the C and T lines, binds to the secondary antibody and coated antigen to form a band. The higher the concentration of the probe, the more it will bind to the secondary antibody or the coating antigen, and the deeper the strip will be formed. Thus, the performance of the test strip is directly affected by the concentration of the detection probe. As shown in Fig. 3. (c), the resuspended PBNPs-mAb is diluted by 0×, 2×,

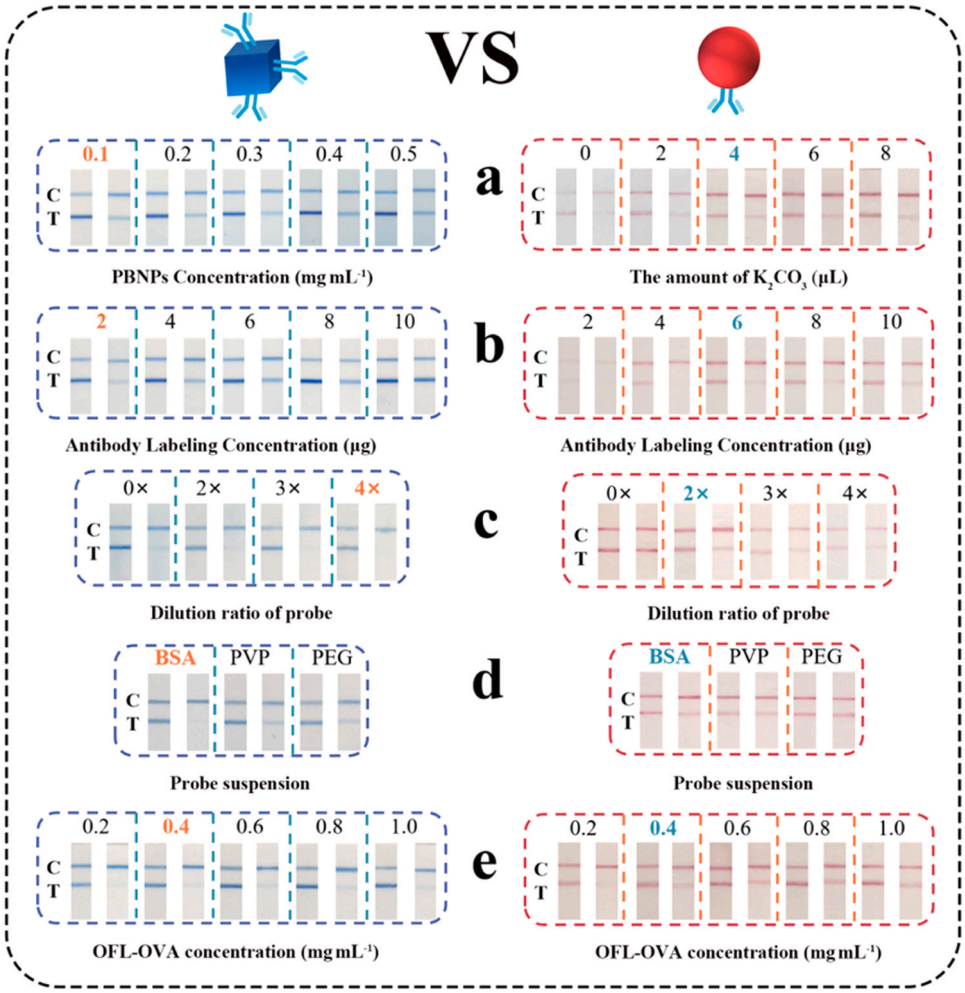

Fig. 3. Optimization results of key parameters of PBNPs-LFIA and AuNPs-LFIA. The left part of the graph is the optimization results of PBNPs-LFIA, and the right part is the optimization results of AuNPs-LFIA. On the left of (a) is the optimization of PBNPs labeling concentration. On the right of (a) is the optimization of the amount of K_2CO_3; (b) is the optimization of antibody labeling concentration; (c) is the optimization of dilution ratio of probe; (d) is the choice of probe suspension; (e) is the optimization of OFL-OVA concentration.

3× and 4× with 0.002 M borate buffer (pH 8.2). When the dilution multiple of the detection probe is 0×, the background color of the test strip is darker, because the aperture of the NC membrane is generally fixed, and the signal labels with higher concentration will block the holes on the NC membrane and accumulate during the flow. An increase in the dilution ratio of the assay probe results in a cleaner base color of the test paper and an increase in sensitivity, so 4× was chosen as the optimal dilution ratio for the assay probe.

3.4.4. Optimization of PBNPs-mAb detection probe suspension

In LFIA assays, researchers usually use resuspensions containing large amounts of proteins or surfactants to re-dissolve the assay probes, whose main function is to stabilize the antibodies (Cavalera et al., 2021; Cai et al., 2023). In this study, probe resuspensions were prepared in 0.002 M (pH 8.2) borate buffer by adding 5 % BSA, PVP-K30, and PEG 20000, respectively. Following the assay procedure in 2.3, PBNPs-mAb was collected and resuspended with three resuspension solutions. As shown in Fig. 3(d), different sensitivities were obtained for the AuNPs-LIFA assay with the three different additives. In this study, we found that when using BSA as an additive, the positive test group had the lightest T line color and the highest test paper sensitivity. On the contrary, when PVP was used as an additive, the T line of the negative control was weaker than the C line and it showed positive results. However, this is obviously not true because at this point the solution does not contain OFL. In order to ensure the accuracy of the experiment, we cannot use the conditions at this point as the best experimental conditions.

3.4.5. Optimization of the original concentration of T line coating

The initial concentration of coated antigen immobilized on the T line during the establishment of the LFIA procedure is also an important factor influencing the sensitivity and color rendition of the T line. The concentration of coating antigen is low, the number of binding with antibody conjugate is small, and the color of T line is light, which may cause false positive results. The higher the concentration of coating antigen, the more antibody conjugate will bind to the coating antigen on the T line, and the color of the T line will be deepened. However, an excessive amount of coated antigen will bind to more PBNPs-mAb to form bands, which will eventually reduce the sensitivity of the test paper. To achieve better sensitivity, we have optimized the concentration of coated antigen on the T line. During the study, five concentration gradients were set as depicted in Fig. 3(e). When the coating concentration is increased from 0.2 mg mL^{-1} to 1.0 mg mL^{-1}, the T line of the blank control group showed deeper blue due to the combination of more and more antibody probes, and the bands of the positive group became deeper and deeper, resulting in lower sensitivity. At the concentration of 0.2 mg mL^{-1}, the T line showed a light blue color due to the low number of bound antibody probes, resulting in a false positive result. To obtain better sensitivity while ensuring good color development, 0.4 mg mL^{-1} was determined to be optimal.

3.5. Optimization of detection conditions of AuNPs-LFIA

3.5.1. Optimization of K_2CO_3 addition amount

AuNPs is a hydrophobic and negatively charged particle. The synthesis of AuNPs-mAb is essentially a process in which protein macromolecules are adsorbed on the AuNPs surface. The mechanism is that the negative charges on the AuNPs surface can combine with the positive charges on the protein surface. When the pH value of AuNPs solution is equal to the isoelectric point of proteins, due to the hydrophobicity of the protein surface will make the gold nanoparticles appear obvious aggregation phenomenon, manifested as a significant deepening of the color, from red to blue or purple. When the pH value of AuNPs solution is lower than the isoelectric point of proteins, protein surface with a positive charge will be neutralized and the gold nanoparticles on the surface of the negative charge, the colloidal gold particles aggregation, manifested as gold nanoparticles from red to grey and black, until they settle. When the pH value of AuNPs solution is too high, the antibody surface has a negative charge, which makes the antibody and the AuNPs with the same negative charge repel each other and can not be combined; in general, only in the conditions that the isoelectric point of the protein is slightly alkaline, the two can be firmly combined (Osman et al., 2018). We varied the pH of the AuNPs solution by adjusting the amount of 0.1 M K_2CO_3 added, setting 0, 2, 4, 6 and 8 μL of K_2CO_3 per mL of AuNPs, respectively. Fig. 3(a) shows that the C and T lines on the test paper became more stable with the addition of K_2CO_3. The color of the bands became clearer and the addition of 4 μL of K_2CO_3 per mL of AuNPS was the optimal condition.

3.5.2. Optimization of particle size

The amount of trisodium citrate added during the synthesis of colloidal gold has a direct effect on the particle size of the colloidal gold and ultimately on the staining properties of the test paper. In general, the more sodium citrate is added, the smaller the particle size of the synthesized AuNPs and the better the stability. On the contrary, the less reducing agent is added, the larger the gold nanoparticles are, the less stable they are, and the easier they are to aggregate and precipitate. We set up three different volumes of trisodium citrate, 0.7 mL, 0.9 mL, and 1.1 mL, respectively, and used UV–vis to scan the spectra of three kinds of AuNPs produced, as shown in Fig. S1(d), and the corresponding maximum absorption wavelengths were obtained as 528 nm, 521 nm, and 519 nm, respectively. according to the particle size formula Y (particle size)=6.0308×λ_{max}-3118.6, the particle sizes of AuNPs were 59 nm, 23 nm, and 17 nm, respectively, and as shown in Fig. S2, when the amount of trisodium citrate was added at 0.9 mL and the particle size was 23 nm, the AuNPs-LFIA had good color rendering and excellent sensitivity, so 23 nm was selected as the optimal particle size.

3.5.3. Optimization of AuNPs labeled antibody concentration

For the concentration of AuNPs-labeled antibodies, we added 2, 4, 6, 8, and 10 μg of antibody to 1 mL AuNPs, respectively. As shown in Fig. 3 (b), when the concentration of antibody labeling is low, the color development of C and T lines in the test paper is not good, and the color development becomes better when the concentration is increased, but too high a concentration will reduce the sensitivity. Considering the amount of reagent, color development effect and sensitivity, 6 μg was selected as the perfect antibody labeling concentration.

3.5.4. Optimization of dilution multiple of AuNPs-mAb detection probe

In this study, four dilution gradients of 0×, 2×, 3× and 4× were selected. As shown in Fig. 3(c), the color development becomes worse as the dilution multiple increases. When the dilution multiple is 2×, the C line and T line bands of the paper are clear in color and highly sensitive, so 2× is selected as the best probe dilution multiple. In addition, when the dilution was 0×, the background color on the test strip did not appear as obvious as that of PBNPs-LFIA, which may be due to the fact that the particle diameter of AuNPs is much less than that of PBNPs, and the antibody-conjugated detection probe flowed smoothly across the NC membrane without causing blockage or aggregation, so the background was relatively clean.

3.5.5. Optimization of AuNPs-mAb detection probe suspension

The specific steps of the test were carried out according to 2.3 and the obtained AuNPs-mAb was resuspended with three resuspensions. As shown in Fig. 3(d), different sensitivities were obtained for the AuNPs-LIFA assay with the three different additives. In this study, we found that when using BSA as an additive, the positive test group had the lightest T line color and the highest test paper sensitivity. On the contrary, when PVP was used as an additive, the T line of the negative control was weaker than the C line and it showed positive results. However, this is obviously not true because at this point the solution does not contain OFL. In order to ensure the accuracy of the experiment,

we cannot use the conditions at this point as the best experimental conditions. When PEG was used, the T line color was darker and the sensitivity was lower in the positive test group. As a result, the researchers selected a probe resuspension solution containing 5 % BSA as the optimal choice.

3.5.6. Optimization of the original concentration of T line coating

The experimental results of AuNPs-LFIA are basically consistent with those of PBNPs-LFIA. Fig. 3(e) show that when the concentration of coating antigen was increased from 0.2 mg mL^{-1} to 1.0 mg mL^{-1}, the T line of the blank control group showed a deeper red color because more and more antibody probes were bound, and the bands of the positive group became deeper and deeper, resulting in lower sensitivity. At a concentration of 0.2 mg mL^{-1}, the T line coating displays a light red band due to the low number of bound antibody probes, resulting in a false-positive outcome. In order to obtain higher sensitivity while ensuring good color development, we chose 0.4 mg mL^{-1} as the optimal concentration of coated antigen.

3.6. Performance Evaluation of PBNPs-LFIA and AuNPs-LFIA

3.6.1. Sensitivity

Under optimal conditions, the standard curves of PBNPs-LFIA and AuNPs-LFIA for the detection of OFL were established. The standard curves were established using the T line signal intensity as the vertical coordinate and the OFL concentration as the horizontal coordinate as illustrated in Fig. 4. The Fig. 4(a) shows the standard curve of PBNPs-LFIA in the detection of OFL. The linear equation is y=-7114.96 lg (x)+16333.79 (R^2=0.989) and the LOD is 0.064 ng mL^{-1}. The IC_{50} of OFL in this detection method is 1.22 ng mL^{-1}; by nonlinear fitting. The

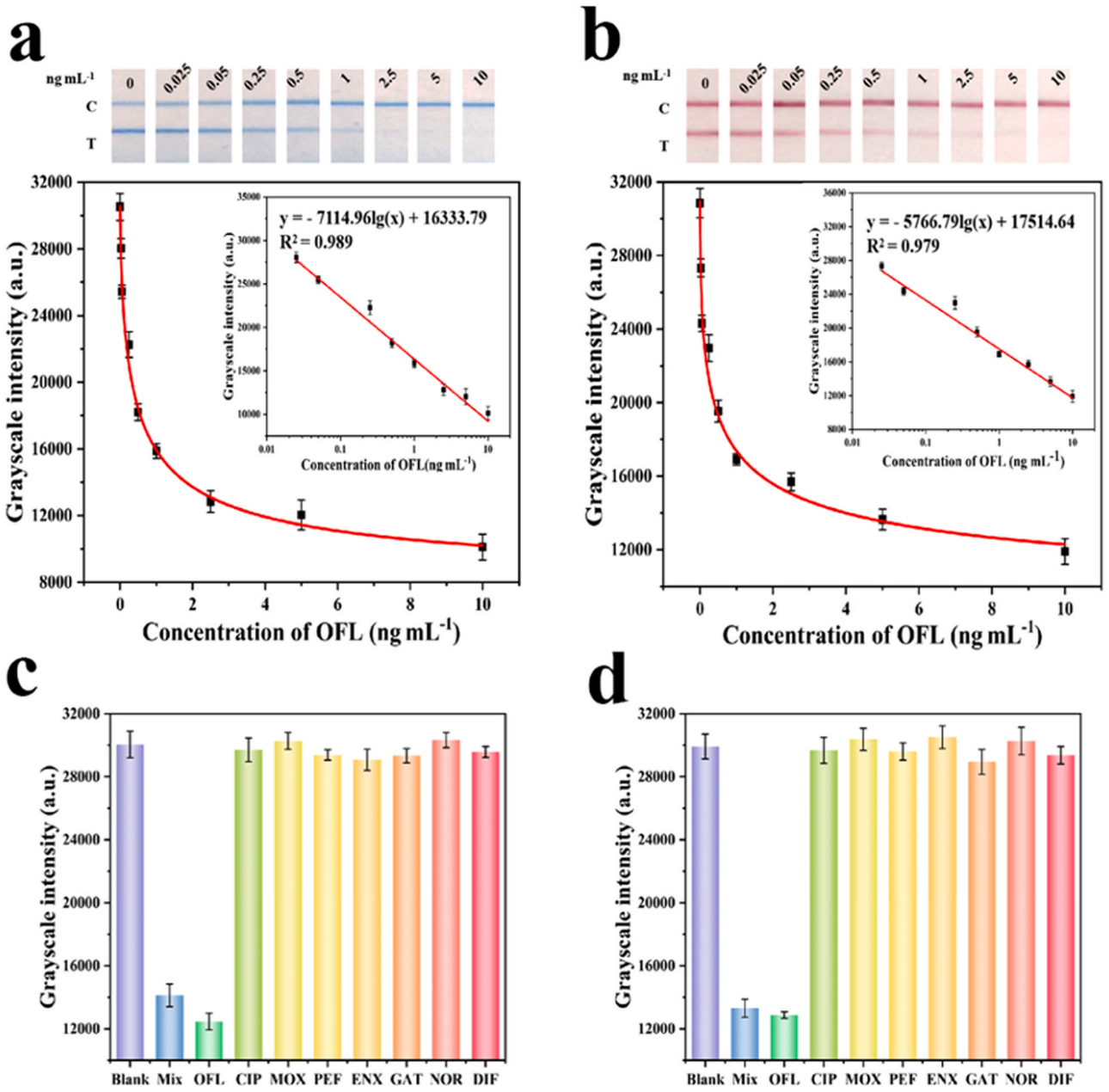

Fig. 4. Detection results of LFIAs. (a) Standard curves of detection of OFL by using PBNPs-LFIA (n=3). (b) Standard curves of detection of OFL by using AuNPs-LFIA (n=3). (c) Specificity results for the PBNPs-LFIA based on the grayscale intensity (n=3). (d) Specificity results for the AuNPs-LFIA based on the grayscale intensity (n=3).

Fig. 4(b) shows the standard curve of AuNPs-LFIA, the linear equation is y=-5766.79 lg(x)+17514.64 (R^2=0.979), and the LOD is 0.147 ng mL^{-1}. The IC_{50} of OFL in AuNPs-LFIA detection method is 2.13 ng mL^{-1} by nonlinear fitting. Both lateral flow immunochromatographic methods showed good linearity in the range of 0.025–10 ng mL^{-1}.The concentration of the standard at which the color of the band becomes significantly lighter to the naked eye is used as the visual detection limit (Misawa et al., 2020). In the actual sample detection process, the visual detection limit (vLOD) of PBNPs-LFIA is 0.05 ng mL^{-1} and the elimination value is 5 ng mL^{-1}. The vLOD of AuNPs-LFIA is 0.25 ng mL^{-1} and the elimination value is 10 ng mL^{-1}.

3.6.2. Specificity

As shown in Fig. 4(c) and Fig. 4(d), when the OFL concentration is 5 ng mL^{-1}, the T line signal intensity of the test strip is obviously lower than that of the blank control group, while the signal strength of the seven fluoroquinolone test groups is basically the same as that of the blank control group. Furthermore, we mixed the OFL standard solution with seven other solutions, which resulted in a decrease in the intensity of the T line signal. The results of the AuNPs-LFIA were in agreement with those of the PBNPs-LFIA. These experimental results demonstrate that both LFIA methods have good specificity for detecting OFL.

3.6.3. Determination of actual samples

Ten random fish samples were purchased from the local market and processed as in 2.7.3, after which OFL was determined in the samples using AuNPs-LFIA, PBNPs-LFIA and HPLC, respectively. The results are shown in Table 1. no OFL was detected in any of the samples.

3.6.4. Accuracy and precision

The accuracy and precision of the two LFIA were evaluated using the recovery rate and coefficient of variation (CV). Table 2 shows that the recovery rate of OFL in fish samples detected by both LFIA types ranged from 84.8 % to 116.3 %, with a CV of less than 10 %. These results indicate that both PBNPs-LFIA and AuNPs-LFIA have high accuracy and precision in detecting OFL in fish samples.

Table 3 summarizes the recently reported methods for OFL detection. Common detection methods include electrochemical, colorimetric, enzyme-linked immunosorbent assay and immunochromatographic methods. Compared with previous studies, our established PBNPs-LFIA and AuNPs-LFIA have wider detection ranges and lower detection limits. However, the electrochemical sensor methods established based on novel nanomaterials also showed better or even more superior detection performance, which may be attributed to the multiple advantages of the nanomaterials themselves such as good biocompatibility and large specific surface area. Therefore, searching for more efficient and superior nanomaterials and applying them to various detection methods will be the way forward.

Table 1
Real samples of fish meat were assayed using PBNPs-LFIA, AuNPs-LFIA and HPLC (n=3).

Sample	PBNPs-LFIA (μg kg^{-1})	CV(%)	AuNPs-LFIA (μg kg^{-1})	CV(%)	HPLC (μg kg^{-1})	CV(%)
fish1	ND	-	ND	-	ND	-
fish2	ND	-	ND	-	ND	-
fish3	ND	-	ND	-	ND	-
fish4	ND	-	ND	-	ND	-
fish5	ND	-	ND	-	ND	-
fish6	ND	-	ND	-	ND	-
fish7	ND	-	ND	-	ND	-
fish8	ND	-	ND	-	ND	-
fish9	ND	-	ND	-	ND	-
fish10	ND	-	ND	-	ND	-

Table 2
Recovery and CV results for fish samples spiked with different OFL concentrations detected using the PBNPs-LFIA and AuNPs-LFIA by measuring the gray-scale intensity (n=3).

Measured	Sample	Spiked (μg kg^{-1})	Mean±SD (μg kg^{-1})	Recovery (%)	CV (%)
PBNPs-LFIA	ND	0.5	0.58±0.05	116.3	0.95
		2.5	2.56±0.21	102.5	1.17
		5	5.32±0.68	106.5	2.09
AuNPs-LFIA	ND	0.5	0.52±0.08	104.0	1.70
		2.5	2.12±0.35	84.8	1.95
		5	4.67±0.58	93.3	1.62

Table 3
Comparison between the present work detecting OFL.

Analytical methods	Sample	Linear range	LOD	Ref
Visualized microarray immunoassay	milk	0.05–12.8 ng mL^{-1}	0.24 ng mL^{-1}	Li et al. (2019)
Electrochemical sensor	eye drops	5.0×10^{-8}-5.0×10^{-4} M	3.7×10^{-8} M	Yang et al. (2022)
Electrochemical sensor	water	0.096–40 μM	0.028 μM	Liu et al. (2023)
AuNPs-LFIA	Chicken	-	10 ng mL^{-1}	Zhu et al. (2008)
AuNPs-LFIA	Milk	-	2 ng mL^{-1}	Sheng et al. (2011)
AuNPs-LFIA	Milk	-	30 ng mL^{-1}	Byzova et al. (2014)
AuNPs-LFIA	Chicken	-	0.089 ng mL^{-1}	Wu et al. (2016)
AuNPs-LFIA	Milk	-	0.1 ng mL^{-1}	Peng et al. (2017)
PBNPs-LFIA	fish	0.025–10 ng mL^{-1}	0.064 ng mL^{-1}	in this study
AuNPs-LFIA	fish	0.025–10 ng mL^{-1}	0.147 ng mL^{-1}	

4. Conclusions

In this study, we synthesized PBNPs and AuNPs using the solvothermal and trisodium citrate reduction methods, respectively. We combined them with anti-OFL mAb to form detection probes and established two kinds of LFIA for detecting OFL in fish. Our research revealed that PBNPs are an excellent signal marker for LFIA. First of all, PBNPs have a unique color compared to traditional AuNPs and have good color rendering during application. Therefore, PBNPs can be used in conjunction with AuNPs to separately label two target-specific antibodies for dual or multiplex detection. Due to the excellent color development of PBNPs, only 1/3 of the amount of antibody labeled with AuNPs is required to achieve the same effect. In addition, the amount of probe used is only 1/2 that of AuNPs-LFIA, resulting in significant cost savings. Meanwhile, the visual detection limit of PBNPs-LFIA was 0.05 ng mL^{-1}, which was 5 folds lower than that of AuNPs-LFIA, and the LOD value was 0.064 ng mL^{-1}, which was 2.3 folds lower than that of AuNPs-LFIA. In conclusion, LFIA using PBNPs is a new method for OFL detection and provides a feasible solution for future trace analysis and multi-detection.

CRediT authorship contribution statement

Yunfeng Zhao: Resources, Data curation, Conceptualization. **Jian Zhang:** Funding acquisition. **Shuangshuang Cui:** Visualization, Validation. **Can Li:** Writing – original draft, Investigation, Formal analysis.

Fengxia Sun: Writing – review & editing, Supervision, Data curation, Conceptualization. **Xiayu Peng:** Writing – review & editing, Supervision.

Declaration of Competing Interest

The authors declare that they have no known competing financial interests or personal relationships that could have appeared to influence the work reported in this paper.

Data availability

Data will be made available on request.

Acknowledgements

The research was supported by the National Natural Science Foundation of China [grant number 32360617], Science Funds of Shihezi University (no. RCZK201920, ZZZC201908A), the Science and Technology Research Project for Shihezi, the eighth Division (no. 2023GY02, 2022PT02), and Bingtuan Science and Technology Program (no. 2021DB016, 2020AB015).

Appendix A. Supporting information

Supplementary data associated with this article can be found in the online version at doi:10.1016/j.jfca.2024.106262.

References

Andreu, V., 2007. Analytical strategies to determine quinolone residues in food and the environment. Trac Trend Anal. Chem. 26 (6), 534–556. https://doi.org/10.1016/j.trac.2007.01.010.

Anfossi, L., Calderara, M., Baggiani, C., Giovannoli, C., Arletti, E., Giraudi, G., 2010. Development and application of a quantitative lateral flow immunoassay for fumonisins in maize. Anal. Chim. Acta 682 (1-2), 104–109. https://doi.org/10.1016/j.aca.2010.09.045.

Busquets, M.A., Estelrich, J., 2020. Prussian blue nanoparticles: synthesis, surface modification, and biomedical applications. Drug Discov. Today 25 (8), 1431–1443. https://doi.org/10.1016/j.drudis.2020.05.014.

Bu, T., Bai, F., Sun, X., et al., 2021. An innovative prussian blue nanocubes decomposition-assisted signal amplification strategy suitable for competitive lateral flow immunoassay to sensitively detect aflatoxin B1. Food Chem. 344, 128711 https://doi.org/10.1016/J.FOODCHEM.2020.128711.

Byzova, N.A., Smirnova, N.I., Zherdev, A.V., et al., 2014. Rapid immunochromatographic assay for ofloxacin in animal original foodstuffs using native antisera labeled by colloidal gold. Talanta 119, 125–132. https://doi.org/10.1016/j.talanta.2013.10.054.

Cai, X., Ma, F., Jiang, J., et al., 2023. Fe-N-C single-atom nanozyme for ultrasensitive, on-site and multiplex detection of mycotoxins using lateral flow immunoassay. J. Hazard Mater. 441, 129853 https://doi.org/10.1016/J.JHAZMAT.2022.129853.

Cavalera, S., Colitti, B., Rosati, S., et al., 2021. A multi-target lateral flow immunoassay enabling the specific and sensitive detection of total antibodies to SARS COV-2. Talanta 223 (1), 121737. https://doi.org/10.1016/j.talanta.2020.121737.

Feng, D., Lu, X., Dong, X., Ling, Y., Zhang, Y., 2013. Label-free electrochemical immunosensor for the carcinoembryonic antigen using a glassy carbon electrode modified with electrodeposited Prussian Blue, a graphene and carbon nanotube assembly and an antibody immobilized on gold nanoparticles. Microchim. Acta 180, 767–774. https://doi.org/10.1007/s00604-013-0985-8.

He, Q., Yang, H., Chen, Y., et al., 2020. Prussian blue nanoparticles with peroxidase-mimicking properties in a dual immunoassays for glycocholic acid. J. Pharm. Biomed. Anal. 187, 113317 https://doi.org/10.1016/j.jpba.2020.113317.

Hendrickson, O.D., Zvereva, E.A., Dzantiev, B.B., Zherdev, A.V., 2023. Highly sensitive immunochromatographic detection of porcine myoglobin as biomarker for meat authentication using prussian blue nanozyme. Foods 12 (23), 4252. https://doi.org/10.3390/foods12234252.

Hu, M., Torad, N.L.K., Chiang, Y.-D., Wu, K.C.W., Yamauchi, Y., 2012. Size- and shape-controlled synthesis of Prussian blue nanoparticles by a polyvinylpyrrolidone-assisted crystallization process. CrystEngComm 14, 3387–3396. https://doi.org/10.1039/C2CE25040C.

Huang, Q., Yang, H., Wang, W., Zhang, Y., 2023. Multi-target photothermal immunochromatography for simultaneous detection of three mycotoxins in foods. Anal. Chim. Acta 1279, 341784. https://doi.org/10.1016/J.ACA.2023.341784.

Jin, Q., Fan, Y., He, T., Peng, J., Liu, J., Wang, J., 2023. Fluorescence polarization assay based on a new recognition motif QepA for the one-step detection of fluoroquinolones in eggs. J. Agric. Food Chem. 71 (49), 19749–19759. https://doi.org/10.1021/ACS.JAFC.3C03526.

Jirachaya, T., Nami, M., Fuangfa, U., Wimonrat, T., P, B.L., Pondpan, S., Flav, K.T., Siriporn, K., Kentaro, K., Hyun, K., Jeewan, T., Chie, N., Yasuhiko, S., 2023. Exploration of the novel fluoroquinolones with high inhibitory effect against quinolone-resistant DNA gyrase of Salmonella Typhimurium. Microbiol Spectr. 11 (6) e0133023-e0133023. 10.1128/SPECTRUM.01330-23.

Juliana, C.-M., L, B.M., E, S.E., M, J.C., Rohan, F., 2019. Prussian blue nanoparticle-based antigenicity and adjuvanticity trigger robust antitumor immune responses against neuroblastoma. Biomater. Sci. 7 (5), 1875–1887. https://doi.org/10.1039/c8bm01553h.

Li, Z., Yao, K., Li, X., 2019. Simultaneous detection of ofloxacin and lomefloxacin in milk by visualized microplate array. J. Food Meas. Charact. 13 (4), 2637–2643. https://doi.org/10.1007/s11694-019-00184-7.

Liao, D., Wang, R., Zheng, Y., Ma, J., Sun, J., Yang, Q., Zhou, G., 2023. In-situ growth of small-size Fe3O4 nanoparticles on N-doped hollow carbon spheres for electrochemical high-efficiency determination of ofloxacin-contaminated water. Microchem J. 191 https://doi.org/10.1016/J.MICROC.2023.108927.

Liang, J., Liu, Z., Fang, Y., et al., 2023. Two kinds of lateral flow immunoassays based on multifunctional magnetic prussian blue nanoenzyme and colloidal gold for the detection of 38 β-agonists in swine urine and pork. Food Chem. 417, 135897 https://doi.org/10.1016/J.FOODCHEM.2023.135897.

Liu, Z., Hua, Q., Wang, J., Liang, Z., Li, J., Wu, J., Shen, X., Lei, H., Li, X., 2020. A smartphone-based dual detection mode device integrated with two lateral flow immunoassays for multiplex mycotoxins in cereals. Biosens. Bioelectron. 158, 112178 https://doi.org/10.1016/j.bios.2020.112178.

Liu, Z., Hua, Q., Wang, J., Liang, Z., Zhou, Z., Shen, X., Lei, H., Li, X., 2022. Prussian blue immunochromatography with portable smartphone-based detection device for zearalenone in cereals, 131008-131008 Food Chem. 369. https://doi.org/10.1016/J.FOODCHEM.2021.131008.

Liu, Z., Wang, Q., Xue, Q., Chang, C., Wang, R., Liu, Y., Xie, H., 2023. Highly efficient detection of ofloxacin in water by samarium oxide and β-cyclodextrin-modified laser-induced graphene electrode. Microchem. J. 186, 108353 https://doi.org/10.1016/J.MICROC.2022.108353.

Misawa, K., Yamamoto, T., Hiruta, Y., Yamazaki, H., Citterio, D., 2020. Text-displaying semiquantitative competitive lateral flow immunoassay relying on inkjet-printed patterns. ACS Sens 5 (7), 2076–2085. https://doi.org/10.1021/acssensors.0c00637.

Nardo, D.F., Chiarello, M., Cavalera, S., Baggiani, C., Anfossi, L., 2021. Ten years of lateral flow immunoassay technique applications: trends, challenges and future perspectives. Sensors 21 (15), 5185. https://doi.org/10.3390/s21155185.

Osman, M.S., Bashah, N.A.A., Amri, N., Kasmir, S.I., Safri, A.I.D., Ariff, M.A.M., Yaakob, N., 2018. Biosynthesis of gold nanoparticles using aqueous extracts of mariposa cristia vespertillonis: influence of pH on its colloidal stability. Mater. Today. Proc. 5 (10), 22050–22055. https://doi.org/10.1016/j.matpr.2018.07.067.

Peng, J., Liu, L., Xu, L., Song, S., Kuang, H., Cui, G., Xu, C., 2017. Nano Res. 10 (1), 108–120. 10.1007/s12274-016-1270-z.

Qiu, Q., Chen, H., Wang, Y., Yin, Y., 2019. Recent advances in the rational synthesis and sensing applications of metal-organic framework biocomposites. Coord. Chem. Rev. 387, 60–78. https://doi.org/10.1016/j.ccr.2019.02.009.

Qin, Z., Li, Y., Gu, N., 2018. Progress in applications of prussian blue nanoparticles in biomedicine. Adv. Health Mater. 7 (20), e1800347 https://doi.org/10.1002/adhm.201800347.

Qureshi, T., Memon, N., Memon, S.Q., Ashraf, M.A., 2016. Decontamination of ofloxacin: optimization of removal process onto sawdust using response surface methodology. Desalin. Water Treat. 57 (1), 221–229. https://doi.org/10.1080/19443994.2015.1006825.

Rana, G.A., Jyotiranjan, B., Ping, X., Subhadeep, G., Taehyun, Y., Kumar, K.S., Hyeock, K.Y., Jung, P.T., 2024. Serodiagnosis of Multiple Cancers Using an Extracellular Protein Kinase A Autoantibody-based Lateral Flow Platform. In: Biosens Bioelectron., 246, 115902 https://doi.org/10.1016/J.BIOS.2023.115902.

Ren, J., Su, L., Hu, H., et al., 2022. Expanded detection range of lateral flow immunoassay endowed with a third-stage amplifier indirect probe. Food Chem. 377, 131920 https://doi.org/10.1016/J.FOODCHEM.2021.131920.

Rodriguez-Mozaz, S., Vaz-Moreira, I., Giustina, S.V.D., Llorca, M., Barceló, D., Schubert, S., Berendonk, T.U., Michael-Kordatou, I., Fatta-Kassinos, D., Martinez, J. L., Elpers, C., Henriques, I., Jaeger, T., Schwartz, T., Paulshus, E., O'Sullivan, K., Pärnänen, K.M.M., Virta, M., Do, T.T., Walsh, F., Manaia, C.M., 2020. Antibiotic residues in final effluents of European wastewater treatment plants and their impact on the aquatic environment. Environ. Int. 140, 105733 https://doi.org/10.1016/j.envint.2020.105733.

Sheng, W., Li, Y., Xu, X., Yuan, M., Wang, S., 2011. Enzyme-linked immunosorbent assay and colloidal gold-based immunochromatographic assay for several (fluoro) quinolones in milk. Mikrochim Acta 173 (3), 307–316. https://doi.org/10.1007/s00604-011-0560-0.

Sunanda, N., Yanxiong, P., Sunitha, T., Kylie, B., Jasmin, F., Yi, X., Bingcan, C., Guodong, L., Y, Q.S., Zhongyu, Y., 2017. Probing the aggregation mechanism of gold nanoparticles triggered by a globular protein. J. Phys. Chem. C. 121 (2), 1377–1386. https://doi.org/10.1021/acs.jpcc.6b11963.

Tian, M., Xie, W., Zhang, T., et al., 2020. A sensitive lateral flow immunochromatographic strip with prussian blue nanoparticles mediated signal generation and cascade amplification. Sens. Actuators. B Chem. 309, 127728 https://doi.org/10.1016/j.snb.2020.127728.

Wang, P., Wang, Z., Su, X., 2015. A sensitive and quantitative fluorescent multi-component immuno-chromatographic sensor for β-agonist residues. Biosens. Bioelectron. 64, 511–516. https://doi.org/10.1016/j.bios.2014.09.064.

Wang, Y., Liu, P., Ye, Y., Hammock, D., Zhang, C., 2023. An integrated approach to improve the assay performance of quantum dot-based lateral flow immunoassays by

using silver deposition. Microchem J. 192, 108932 https://doi.org/10.1016/J.MICROC.2023.108932.

Wolfgang, H., K, T.N.T., Jenny, A., G, F.D., 2007. Determination of size and concentration of gold nanoparticles from UV–vis spectra. Anal. Chem. 79 (11), 4215–4221. https://doi.org/10.1021/ac0702084.

Wu, Y., Guo, S., Dong, Q., Song, Y., 2016. Development of an immunochromatographic test strip for rapid simultaneous detection of enrofloxacin and ofloxacin in tissue of chicken muscle and pork. Food Anal. Methods 9, 2807–2813. https://doi.org/10.1007/s12161-016-0474-x.

Yang, D., Deng, Z., Wang, S., Yin, X., Xi, J., Andersson, M., Wang, J., Zhang, D., 2023. Polydopamine-coated two-dimensional nanomaterials as high-affinity photothermal signal tag towards dual-signal detection of Salmonella typhimurium by lateral flow immunoassay. Chem. Eng. J. 472, 145110 https://doi.org/10.1016/J.CEJ.2023.145110.

Yang, Z., Hu, J., Zhang, X., Yang, H., Meng, P., Zhang, H., Sun, Y., 2022. MXene-based composites as an electrochemical sensor for ultrasensitive determination of ofloxacin. Anal. Bioanal. Chem. 415 https://doi.org/10.1007/S00216-022-04402-Y.

Yin, X., Liu, S., Kukkar, D., Wang, J., Zhang, D., Kim, K., 2024. Performance enhancement of the lateral flow immunoassay by use of composite nanoparticles as signal labels. Trac Trend Anal. Chem. 170, 117441 https://doi.org/10.1016/J.TRAC.2023.117441.

Zakaria, M.B., Belik, A.A., Liu, C.H., Hsieh, H.Y., Liao, Y.T., Malgras, V., Yamauchi, Y., Wu, K.C.W., 2015. ChemInform abstract: Prussian blue derived nanoporous iron oxides as anticancer drug carriers for magnetic-guided chemotherapy. ChemInform 46 (42). https://doi.org/10.1002/chin.201542218.

Zhang, D., Li, P., Zhang, Q., Zhang, W., 2011. Ultrasensitive nanogold probe-based immunochromatographic assay for simultaneous detection of total aflatoxins in peanuts. Biosens. Bioelectron. 26 (6), 2877–2882. https://doi.org/10.1016/j.bios.2010.11.031.

Zhang, H., Zhang, W., Gao, X., Man, P., Sun, Y., Liu, C., Li, Z., Xu, Y., Man, B., Yang, C., 2019. Formation of the AuNPs/GO@MoS2/AuNPs nanostructures for the SERS application. Sens. Actuators. B Chem. 282, 809–817. https://doi.org/10.1016/j.snb.2018.10.095.

Zhang, T., Ma, X., Zhang, D., Xu, Z., Ma, M., Shi, F., 2022. Rapid vertical flow technique for the highly sensitive detection of Brucella antibodies with Prussian blue nanoparticle labeling and nanozyme-catalyzed signal amplification. World J. Microbiol Biotechnol. 39 (1), 23. https://doi.org/10.1007/S11274-022-03462-7.

Zhao, B., Huang, Q., Dou, L., et al., 2018. Prussian blue nanoparticles based lateral flow assay for high sensitive determination of clenbuterol. Sens. Actuators. B Chem. 275, 223–229. https://doi.org/10.1016/j.snb.2018.08.029.

Zhong, Y., Chen, Y., Yao, Y., Zhao, D., Zheng, L., Liu, G., Ye, Y., Chen, W., 2016. Gold nanoparticles based lateral flow immunoassay with largely amplified sensitivity for rapid melamine screening. Microchim. Acta 183 (6), 1989–1994. https://doi.org/10.1007/s00604-016-1812-9.

Zhu, Y., Li, L., Wang, Z., et al., 2008. Development of an immunochromatography strip for the rapid detection of 12 fluoroquinolones in chicken muscle and liver. J. Agric. Food Chem. 56 (14), 5469–5474. https://doi.org/10.1021/jf800274f.